(Accepted by the journal "Nanotechnology," Oct 26, 2009)

Very Long Single and Few-walled Boron Nitride Nanotubes via the Pressurized Vapor/Condenser Method

Michael W. Smith[1], Kevin C. Jordan[2], Cheol Park[3], Jae-Woo Kim[3], Peter T. Lillehei[1], Roy Crooks[3], Joycelyn S. Harrison[4]

Affiliations:
[1]NASA Langley Research Center, Hampton, VA 23681, USA.
[2]Thomas Jefferson National Accelerator Facility, Newport News, Virginia 23606, USA.
[3]National Institute of Aerospace, 100 Exploration Way, Hampton VA 23666, USA.
[4]Air Force Office of Scientific Research, Washington, DC.

E-mail:
(synthesis) Michael.W.Smith@NASA.gov
(analysis) Cheol.Park-1@NASA.gov

Abstract

A new method for producing long, small diameter, single and few-walled, boron nitride nanotubes (BNNTs) in macroscopic quantities is reported. The pressurized vapor/condenser (PVC) method produces, without catalysts, highly crystalline, very long, small diameter, BNNTs. Palm-sized, cotton-like masses of BNNT raw material were grown by this technique and spun directly into centimeters-long yarn. Nanotube lengths were observed to be 100 times that of those grown by the most closely related method. Self-assembly and growth models for these long BNNTs are discussed.

1. Introduction

Boron nitride nanotubes (BNNTs) are desired for their exceptional mechanical, electronic, thermal, structural, textural, optical, and quantum properties. Golberg et al., [1] gives a detailed review of possible applications for BNNTs. To date, BNNTs have been grown by a number of techniques which can be divided into two broad categories based on the class of material produced and the temperature employed. One is the high temperature category in which energy is concentrated into a boron (B) or boron nitride (BN) target at a level which can vaporize elemental boron. BNNTs form when the liberated vapors react with nitrogen and condense into solid state. This energy can be provided by a laser [2-6] or generated by an arc discharge [7-9]. Only small quantities (milligrams) of material have been produced by this high temperature method, but the tubes are of high quality. High temperature BNNTs are highly crystalline, have one or just a few walls, and most importantly, the tube walls have few defects and are parallel to the axis of the nanotube. The second broad category of BNNT synthesis is the low temperature method, applied between 600 °C and 1700 °C, well below the vaporization temperature of pure B (over 4000 °C, depending on ambient pressure). The low

temperature synthesis methods include ball-milling and chemical vapor deposition (CVD). In ball-milling, finely-milled precursor powders of B and catalyst are annealed in an N_2 or ammonia gas atmosphere, sprouting nanostructures on their surfaces [10-13]. In CVD, a B-containing vapor, for example B_2O_2, reacts with a nitrogen-containing gas, for example ammonia, to deposit nanostructures on a substrate placed in a furnace [14-16]. Hundreds of milligrams to grams of raw material can be produced by ball-milling and CVD and the nanostructures contain a very high fraction of hexagonal BN (h-BN). However, typical diameters of CVD and ball-mill BNNTs are about an order of magnitude greater than those grown by high-temperature techniques (~50 nm, vs. ~5 nm) and these tubes frequently have wavy walls, elbows, herringbone, or bamboo-like morphologies.

In this paper we introduce a new high temperature synthesis technique which is scalable to gram quantities, and preserves the desirable morphology of a small diameter, few-walled tube. In addition, the technique produces tubes of extraordinary length, giving the raw material the appearance of conventional textile fibers. This appearance is further reinforced by natural, macroscopic alignment of the as-grown material, facilitating new processing paths, for instance the spinning of yarns, which is demonstrated.

2. Experimental Method

Fig. 1 is a schematic representation of the technique we call the pressurized vapor/condenser (PVC) method. The elements of this cartoon were derived from particle scattering video of the PVC device in operation. The technique involves the forced condensation of seed particles in an ascending plume of pure boron vapor held at elevated ambient pressure. The boron vapor is produced at a quasi-point source by local heating of a target centered in the chamber. The large density difference between the hot boron vapor (over 4000 C) and the surrounding high pressure N_2 gas (room temperature) generates a strong buoyancy force and a narrow vertical plume of boron vapor with a velocity profile as shown in Fig. 1A. When a cooled metal wire traverses the boron plume as indicated in Fig. 1B, the wire acts as a condenser and leaves boron droplets in its wake by homogeneous nucleation. Because there is no N_2 in the core of the plume, no BN forms at this time. Milliseconds later (Fig. 1C.), the boron droplets have translated upward to form a loop which is shaped by the velocity profile of the boron plume. Tens of milliseconds after that, the droplets begin to encounter N_2 gas that has mixed with the boron plume by diffusion through the shear layer surrounding the plume. The N_2 diffusion is indicated by the red arrows in Fig. 1D. Now that both reactants B and N_2 are present and nucleation sites in the form of B droplets are present, BNNTs can form. Growth of the BNNTs proceeds quickly at elevated pressure, as the molecular collision rate is proportional to the ambient pressure. Clusters of BNNT grow, intermingle, interlock, and are shaped by fluid shear into a dimensionally stable fibril shape, all in about 100 ms (Figs. 1 E. and F.). Although elastic particle scattering is not species specific, i.e. one cannot distinguish B from BN in the videos; one can distinguish free particles from those that are interlocked in a fibril. The 'loop' of droplets and clusters in Fig. 1A-D is readily deformed by the flow of the buoyant plume; the final fibril is of

fixed length and appears in the video visualizations as a thread, or streamer, attached by one end to the condenser, giving the appearance of a flag flapping in the wind.

The PVC technique can be employed with many variations. The heat source, the target material, the pressure, and the condenser material and geometry can take numerous forms. In the current work, PVC synthesis runs were conducted at N_2 pressures between 2 and 20 times atmospheric pressure. Boron vapor was produced with two different heating sources: a 1 kW free electron laser [17] operating at a wavelength of 1.6 μm and a kW-class commercial welding laser operating at 10.6 μm. Successful target materials included hot-pressed BN, cold-pressed BN, amorphous B powders and cast B. Successful condensers were made from BN, B, stainless steel, copper, niobium, and tungsten in various forms of surfaces, wires, sheets, ribbons, and rods. No catalyst was ever employed and the wide variety of successful condenser surfaces demonstrated that the condenser simply acted as a cooler and not a catalytic surface.

3. Results and Discussion

A typical fibril grown by the PVC scheme outlined in Fig. 1 was approximately 1 mm in diameter by 10 cm in length. Such fibrils could be grown in a continuous assembly line by repeatedly intercepting the B plume with a moving condenser. **Fig. 2** shows the results of such a production run. This 60 mg mass of many individual BNNT fibrils was produced by translating the metal condenser about 20 cm over the course of about 30 minutes of continuous running. In Fig. 2, the fibrils exhibit natural alignment along the axis of growth, giving the raw material the appearance of combed cotton. The process of fibril formation is efficient, as the mass of the BNNT raw material is typically equal to around 80% of the mass loss of the boron source target.

In **Fig. 3A** a 200 mg sample of as-grown PVC-BNNT material is shown. The material has an unusually low density. In the current case 200 mg fills a 10 cm by 10 cm jar, indicating that the PVC-grown BNNT product has a much higher surface area than previously available (e. g. by ball-mill or CVD techniques).

Carbon nanotube (CNT) yarns have been reported, spun from 100 μm long CNT arrays, CVD forests, or fibrils [18-21]. Analogous to CNT yarns we report a BNNT yarn, the first to our knowledge. As shown in **Fig. 3B**, it was about 3 cm in length and spun directly from PVC-grown BNNT raw material. A group of fibrils weighing about 10 mg (representing ~5 minutes of synthesis time) was separated from a mass of raw material, drawn slightly in the growth direction, and finger-twisted to form a simple one-ply yarn with a twist angle of about 45 degrees. Before twisting, the mass of fibrils was delicate to the touch with little mechanical strength. After twisting, the same mass of material could readily support a small load (a ~6 g coin), clearly demonstrating the structural reinforcement due to spinning.

A measurement of the length of the tubes composing the yarn was of great interest. Since BNNTs have a band gap around 5.5 eV, they are not sufficiently conductive to be imaged by SEM when they are separated as individual tubes. So, for a direct measurement of tube length PVC-BNNTs were mixed into a special polymer matrix, and then imaged by

SEM (to be shown in a future report). BNNT bundles only a few nanometers in diameter and at least 100 μm long were seen at a fracture surface in the polymer matrix. The ends of such tube bundles were not visible at the fracture surface, being buried deep in the polymer. Thus, the full length of the bundles could not be determined by this technique, though lengths much greater than 100 μm were implied.

Although a direct measurement of total BNNT length was not made with in-polymer imaging, an estimate can be derived by considering the nature of staple fibers in yarns. The manner in which staple fibers are spun to produce strong yarns is understood theoretically [19]. Longer staple fibers produce stronger yarns, as does more friction between staple fibers and smaller yarn diameters. Spinning does little to increase mechanical strength if the staple fiber length to yarn diameter ratio drops to unity. No reinforcing effect occurs unless the staple fibers are long enough to lock around each other. So, because the current BNNT staple fibers can successfully be spun into 1 mm diameter yarns, a length of at least 1 mm is implied. To bracket this comparison, commercial cotton thread is spun from staple fibers with an average length of around 28 mm's [22]. The current BNNT yarn has an intermediate strength between zero and that of cotton thread. So by crude interpolation, one can expect a staple BNNT length of at least several millimeters.

It should be noted that the BNNT yarn is presented not to suggest its immediate practical application, but to demonstrate a unique property of PVC-grown BNNT material. Considerable improvement in a practical yarn can be expected through a more refined spinning process that includes purifying the raw material to increase frictional locking and smaller, tighter plies. However, even in its current form this is a notable development as for many applications a fabric or macroscopic fiber is an advantageous form—armor, spacesuits, and aerospace structural layups, for instance. For these, the ready processing of PVC-BNNTs by textile techniques suggests considerable opportunity.

For other applications high temperature and oxidation resistance will be of paramount importance, for example for spaceflight re-entry heat shields or jet engine parts. To this end, the thermal stability of raw PVC-BNNTs was studied with a thermogravimetric analyzer (TGA). **Fig. 4** shows TGA spectra of PVC-BNNTs in air and nitrogen, respectively. The BNNT tubes were stable even up to 1000°C with slight weight gain because of oxidation in air. For comparison, CNTs are completely decomposed above 400°C in air. The left inset in Fig. 4 shows the oxidized BNNTs remaining after the TGA run in air; the right inset reveals details of these oxidized BNNTs at higher magnification. The gained weight above 800°C was determined by FTIR to be B_2O_3 (as also observed by Han et al. [23]). The possibility that the oxidation only affects the outer layer of multi-wall BNNTs is interesting and worthy of investigation, as such a layer may act as a protective coating in high temperature applications.

Next, nanoscale properties if the PVC-BNNTs are reported. **Figs. 5A-D** show the raw material under increasing levels of magnification. In Fig 5A, a scanning electron microscope (SEM) image of a short section of a single as-grown BNNT fibril is shown.

The fibril, about 1 mm wide, is composed of a number of aligned, distinct, vertical strands which extend the full height of the image, indicating that the raw material has a preferential alignment axis parallel to the growth direction (indicated by the white arrow). Along the growth axis, the raw material is highly elastic. Transverse to the growth axis, the material is easily separated into individual strands with light mechanical force. On the micron and sub-micron scale (Figs. 5B and C), the as-grown BNNT material is an entangled network of long, branching nanotubes and tube bundles, often linked at nodes anchored by nanodroplets. On these SEM images the tubes are light colored and the droplets dark. The less conductive BNNT and tube bundles appear brighter than the more conductive boron metalloid droplets. As seen in Figs 5B and C, the ratio of white tubes to dark droplets, one measure of purity, is very high. Further analysis by energy filtered TEM and elemental mapping showed that the dark droplets were elemental B while the white tubes were composed of B and N in the form of BNNTs. Round droplets caged in layers of polygonized BN were frequently seen at termination points in the network as well. Fig. 5D shows several selected tubes under high resolution TEM. The coaxial walls are straight and parallel to the axis of the tube with well-defined uniform inner and outer diameters. Single-wall BNNTs can be found, but the most common number of walls is between 2 and 5, inclusive.

In **Fig. 6**, an 8-walled tube is shown at still higher magnification. Eight-walled PVC tubes are rare, but even at this large diameter, all 8 walls are smooth and parallel to the axis of the tube and the uniform wall spacing is measured to be about 0.34 nm. Parallel, regularly spaced walls are indicative of a high level of crystallinity, as they are only expected to occur when the h-BN walls are defect-free. A representative electron energy loss spectroscopy (EELS) plot derived from this 8-walled tube is shown in the inset of Fig. 6. The BN composition, derived by normalizing several spectra against a BN standard, was repeatedly found to be 1:1, confirming that the imaged tubes are boron nitride.

Fig. 7 shows an electron diffraction pattern for a sample of PVC-BNNT raw material. The sample region was a 200 nm by 200 nm cross section through un-purified clump of BNNT captured on a grid. The volume encompassed a small cluster of non-oriented BNNTs and some particulate impurities. The peaks for the BNNT sample were readily identified and matched with those of an h-BN standard. This match confirms the hexagonal BN lattice structure of the BNNTs, the interwall spacing (about .34 nm), and the general purity of the sample.

The nanoscale imaging and analysis provided in Figs. 5 and 6 directly support the macroscopic observations and visualizations described in Fig. 1. Namely, that in the PVC technique, liquid droplets of boron serve as nucleation sites for the growth of a network of BNNT tubes and bundle clusters which grow rapidly and interlock to form fibrils.

These observations are also in considerably agreement with the nanoscale root-growth mechanism for high-temperature-synthesized BNNTs described by Arenal et al. [6]. In particular, they observed growth of individual tubes and bundles from round liquid boron

nanoparticles coated with cages of BN. But, in contrast to the PVC case, their experiments were carried out at low ambient pressure (sub-atmospheric) and the boron droplets formed only through natural cooling. These appear to be the two critical differences which inhibit the growth of very long BNNTs. Although further species-specific measurements will be required to provide verification, the particle scattering visualization and the analysis of the PVC BNNT raw material suggest that PVC tubes grow longer for two reasons. One, there is a longer residence time for seed particles in the reaction zone, both because the reaction zone is elongated in the PVC geometry and because forced condensation of the seed particles upstream of the reaction zone maximizes the available transit time. And two, BN formation occurs at a higher rate in the PVC technique because the molecular collision rate is proportional to the chamber pressure. In summary, relatively long tubes form when a relatively high B-N reaction rate is sustained over a relatively long time. The self-assembly mechanism appears to be the same as observed by Arenal, but it is accelerated and prolonged in the PVC scheme.

5. Conclusions

We have demonstrated a new and conceptually simple method of producing extraordinarily long, highly crystalline BNNTs in bulk called the PVC method. New clues to the nature of BNNT growth were gleaned from this unique production method and used to extend an existing model of self-assembly. The BNNTs formed by the PVC method have three important characteristics. One, they grow without catalyst using only B and N_2 as the reactants, eliminating the need to use acid or other destructive purification treatments to remove metals or carbon. Two, they have natural alignment on the macroscopic scale, producing an as-grown appearance similar to cotton fiber. This allows them to be processed with well-known textile techniques as demonstrated by the spinning of yarn. And three, and most importantly, they are highly crystalline with small diameters and extraordinary lengths. Such a morphology can be expected to fulfill many theoretical predictions of desirable mechanical, electronic, thermal, optical, piezo, and electronic properties, in practical applications.

Acknowledgements

This work was supported in part by the NASA Langley Creativity and Innovation Program, the NASA Subsonic Fixed Wing program, Thomas Jefferson National Accelerator Facility (DOE contract number DE-AC05-06OR23177), and The Commonwealth of Virginia. Special thanks to the FEL Division of JLab for hosting the experiments.

[1] D. Golberg, Y. Bando, C. C. Tang, C. Y. Zhi, *Adv. Mater.*, **2007**, *19*, 2413.

[2] D. Golberg, A. Rode, Y. Bando, M. Mitome, E. Gamaly and B. Luther-Davies, *App Phys Lett.* **1996**, *69*, 2045-2047.

[3] T. Laude, Y Matsui, A. Marraud, B. Jouffrey, Appl Phys Let. **2000**, *76*, 3239.

[4] T. Laude, thesis Ecole Centrale Paris. Boron Nitride Nanotubes Grown by Non-Ablative Laser Heating: Synthesis, Characterization and Growth Process, **2001**.

[5] R. S. Lee, J. Gavillet, M. Lamy de la Chapelle, A. Loiseau, J.-L. Cochon D. Pigache, J. Thibault, F. Willaime, *Phys Rev B.* **2001**, *64,* 121405-1.

[6] R. Arenal, O. Stephan, J-L. Cochon, A. Loiseau,. *J. Am. Chem. Soc.* **2007**, *129*, 16183-16189.

[7] Nasreen G. Chopra, R. J. Luyken, K. Cherrey, Vincent H. Crespi, Marvin L. Cohen, Steven G. Louie, and A. Zettl, *Science*, **1995,** *269.* 966 – 967.

[8] M. V. P. Altoe, J. P. Sprunck, J.-C. P. Gabriel, K. Bradley, *J. of Mat. Sci.,* **2003**, *38,* 4805.

[9] C. M. Lee et al., *Current App Phys.* **2005**, *6*, 166.

[10] J. Hurst and Gorican Developments in Advanced Ceramics and Composites: Ceramic Engineering and Science Proceedings, *26*, 8.

[11] Narottam P. Bansal and Janet B. Hurst Sung R. Choi, NASA/TM—2005-213874

[12] Jun Yu, Bill C. P. Li, and Ying Chen, *J. of Mat. Sci.* **2007**, 42, 4025.

[13] Hua Chen , Ying Chen, Yun Liu, Lan Fu, Cheng Huang, David Llewellyn, Chem. Phys. Lett. **2008**, *463*, 130.

[14] Chunyi Zhi, Yoshio Bando, Chengchun Tan and Dmitri Golberg, *Solid State Communications,* **2005**, *135*, 67.

[15] Jiesheng Wang, Vijaya K. Kayastha, Yoke Khin Yap, Zhiyong Fan, Jia G. Lu, Zhengwei Pan, Ilia N. Ivanov, Alex A. Puretzky, and David B. Geohegan, *Nano Lett.*, **2005**, *5* (12), 2528.

[16] Chee Huei Lee, JieshengWang, Vijaya K Kayatsha, Jian Y Huang and Yoke Khin Yap, *Nanotechnology,* **2008**, *19*, 455605.

[17] G. R. Neil, C. Behre, S. Benson, M. Bevins, G. Biallas, J Boyce, J Coleman, L. A. Dillon-Townes, D. Douglas, H. F. Dylla, R. Evans, A. Grippo, D Gruber, J. Gubeli, D. Hardy, C. Hernandez-Garcia, K Jordan, M. Kelley, L. Merminga, J. Mammosser, W. Moore, N. Nishimori, E. Pozdeyev, J Preble, R. Rimmer, M. Shinn, T. Siggins, C. Tennant, R Walker, G. P. Williams, S. Zhang, *Nuclear Instr. and Methods in Phy. Res.,* **2006,** *A557*, 9.

[18] L. X. Zheng, M. J. O'Connell, S. K. Doorn, X. Z. Liao, Y. H. Zhao, E. A. Akhadov, M. A. Hoffbauer. *Nature Materials,* **2004**, ***3,*** 673.

[19] Mei Zhang, Ken R. Atkinson, Ray H. Baughman. *Science*, **2004**, *306*, 1358.

[20] Qingwen Li, Xiefei Zhang, Raymond F. DePaula, Lianxi Zheng, Yonghao Zhao, Liliana Stan, Terry G. Holesinger, Paul N. Arendt, Dean E. Peterson, and Yuntian T. Zhu *Adv. Mat.* **2006**, *18*, 3160.

[21] Kaili Jiang, Qunqing Li, Shoushan Fan, *Nature,* **2002**, ***419***, 801.

[22] National Cotton Council of America, Cordova, TN, 38016.

[23] W.-Q. Han, W. Mickelson, J. Cumings, A. Zettl, *Appl. Phys. Lett.* **81**, 1110 (2002)

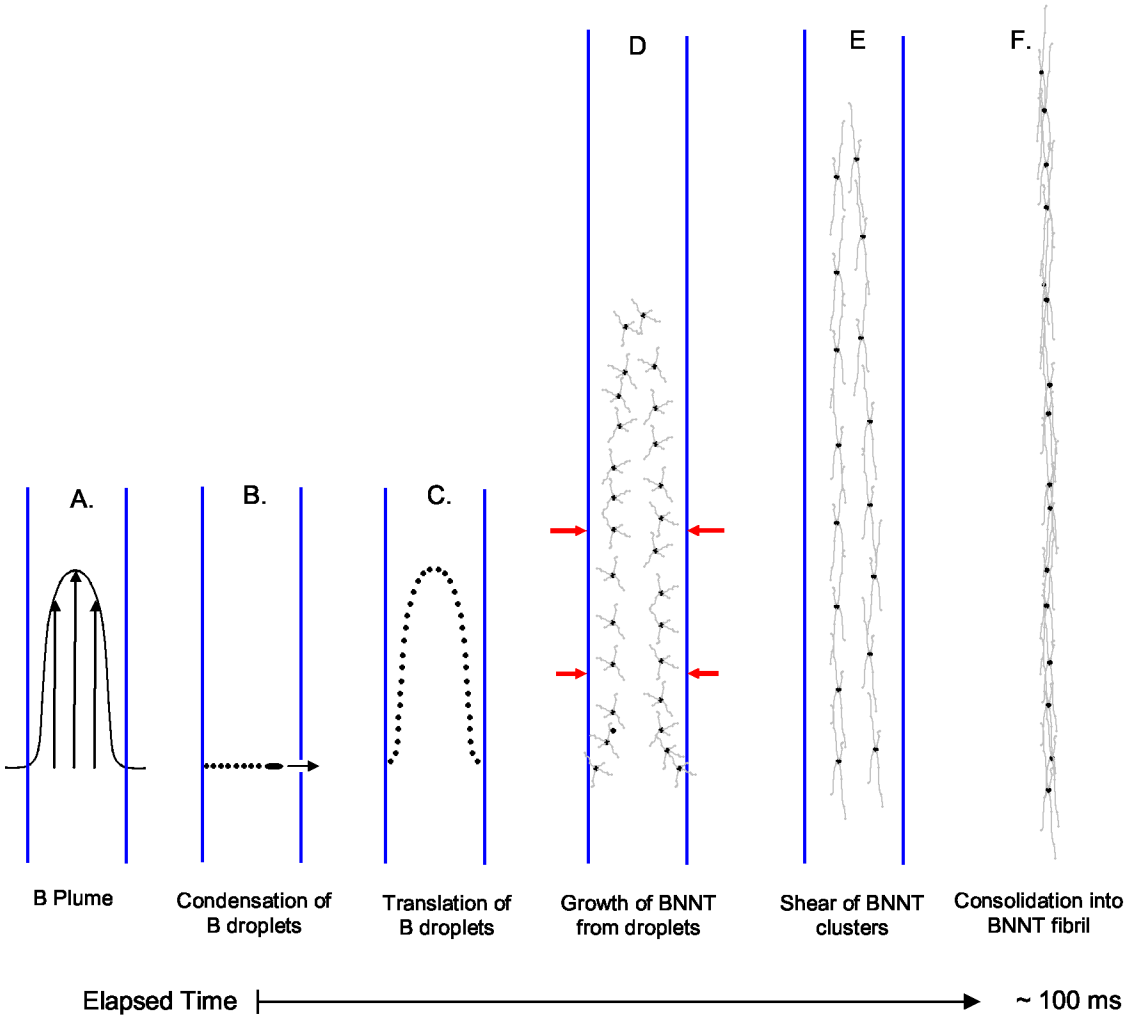

Figure 1. Schematic showing the stages of growth of BNNT fibrils via the PVC method. A.) Velocity profile of the buoyant boron vapor plume (not to scale). B.) Condenser (metal wire normal to the page, indicated by small arrow) traverses plume, leaving trail of boron droplets in its wake. C.) Droplets translate downstream (downstream = up in this case), in accordance with the velocity profile. D.) BNNTs nucleate and grow from droplets. E.) Growth continues as BNNT clusters shear in the flow and begin to interconnect. F.) Fibril takes its final shape as BNNT clusters consolidate into single networked structure.

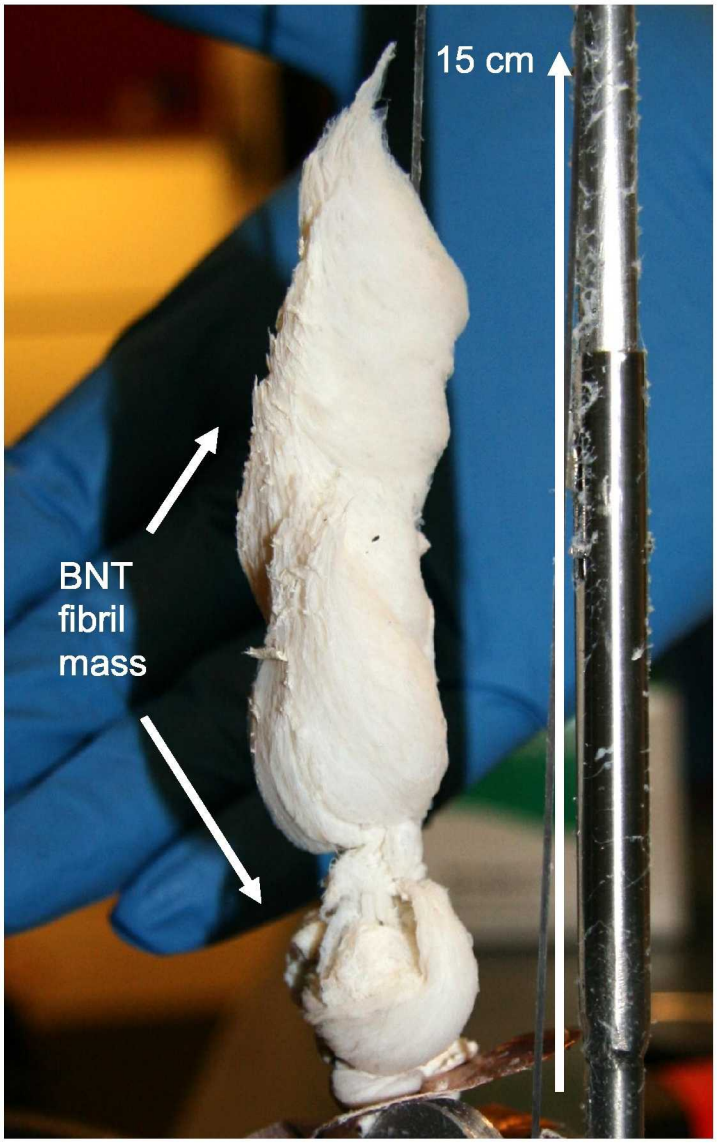

Figure 2. The results of a 200 mg PVC BNNT production run. The unprocessed material has the appearance of cotton balls, though the texture is somewhat softer and the material finer-grained.

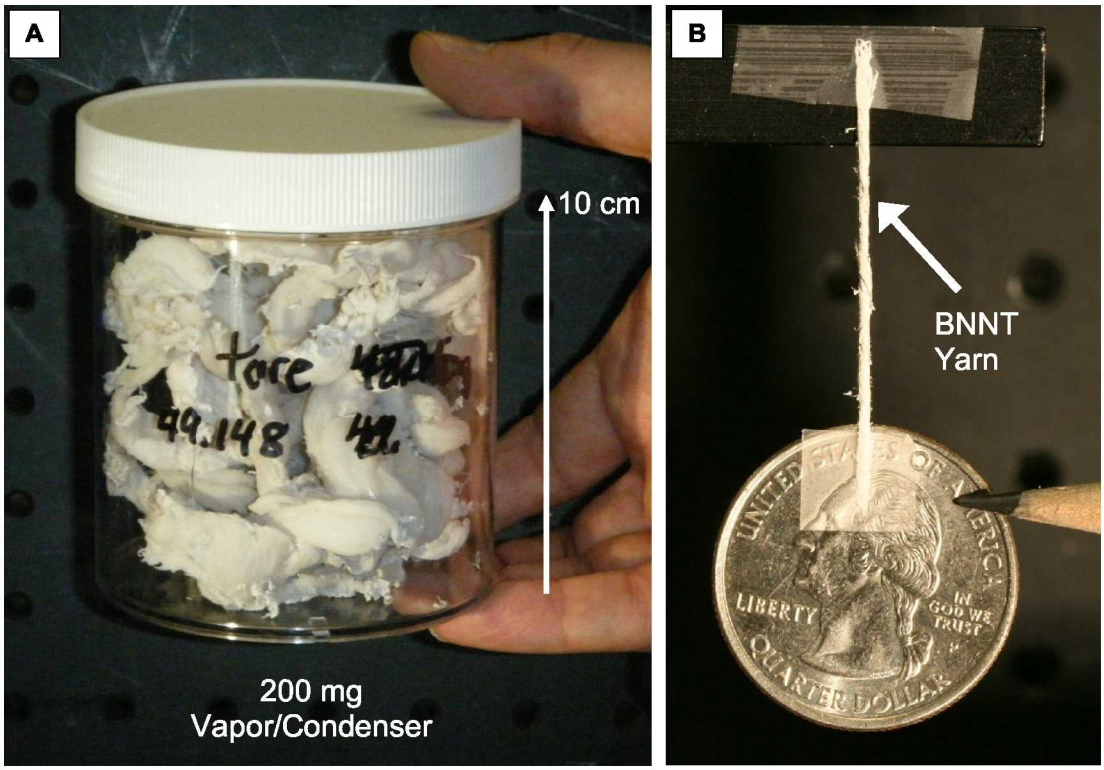

Figure 3. A.) 200 mg of PVC-grown BNNT raw material and yarn. B.) A ~1 mm diameter, 3 cm long BNNT yarn spun directly from PVC-grown BNNT raw material.

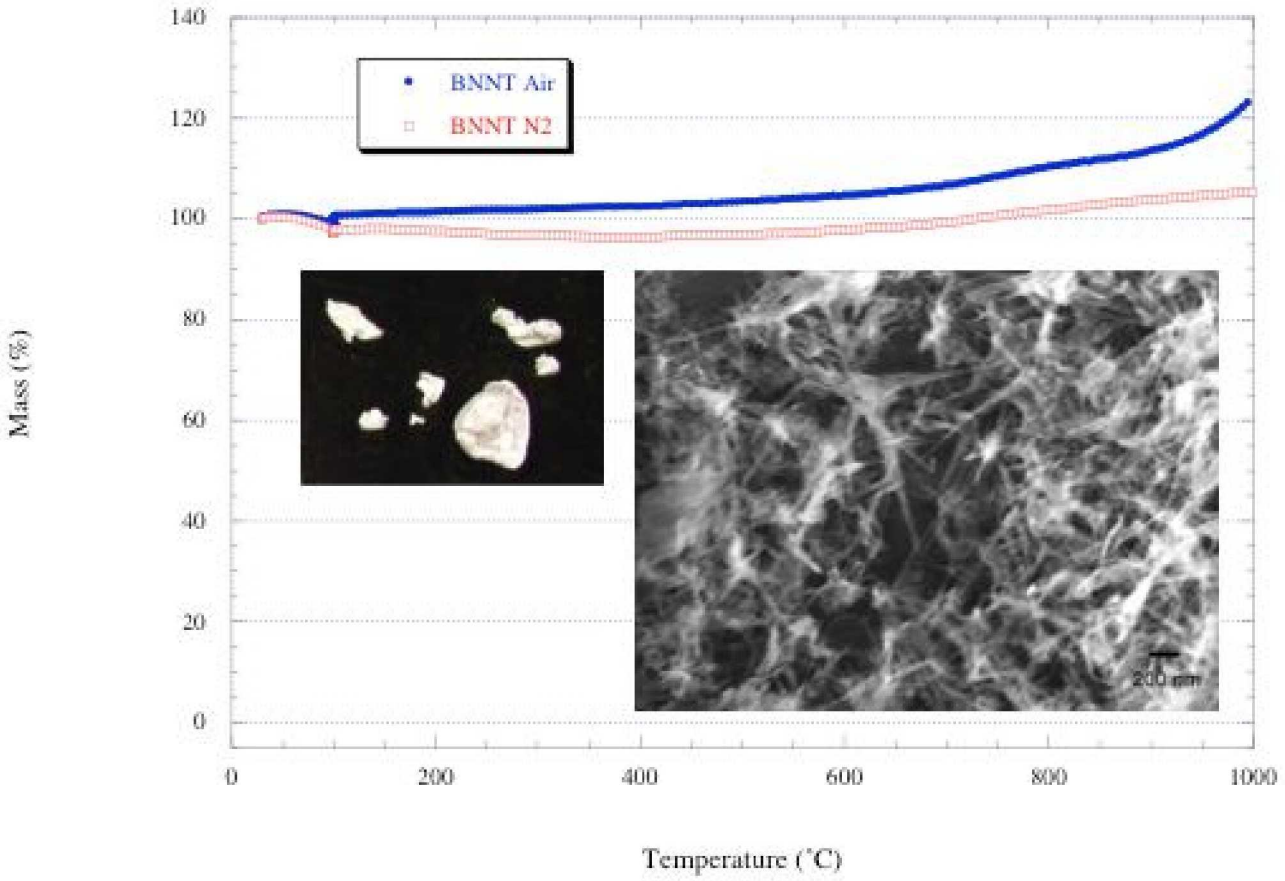

Figure 4. Thermogravimetric analysis showing the stability of PVC-BNNTs at high temperature. Insets show the resulting product after heating to 1000 C at low (left) and high (right) magnification.

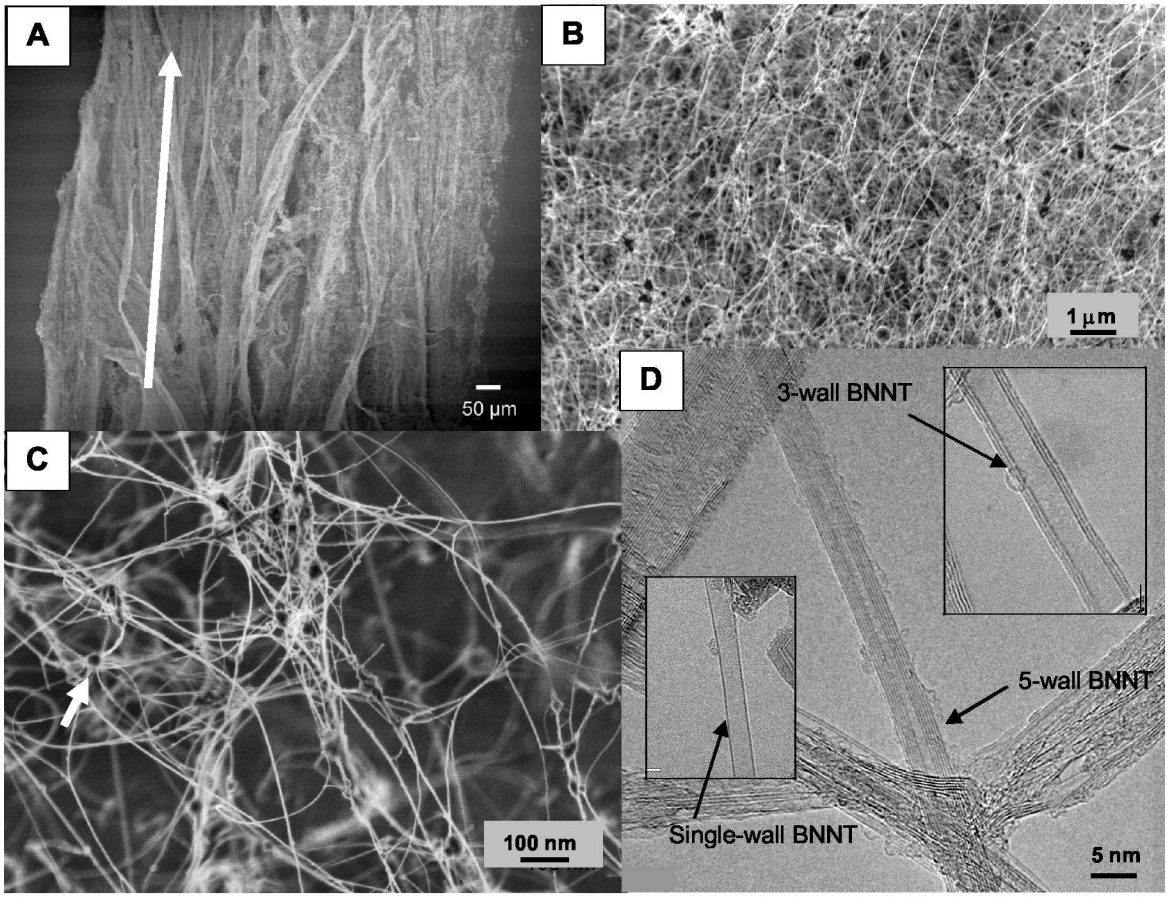

Figure 5. Scanning (A-C) and transmission (D) electron microscope images showing the structure of PVC-grown BNNT fibrils at increasing magnifications. A.) The growth direction, parallel to the BNNT fibrils, is indicated by the white arrow. C.) An arrow marks a round, solidified boron droplet. D.) Typical 1, 3, and 5 wall tube are shown. Although as many as 8 walls have been observed (see Fig. 6), 2 to 5 walls are most common.

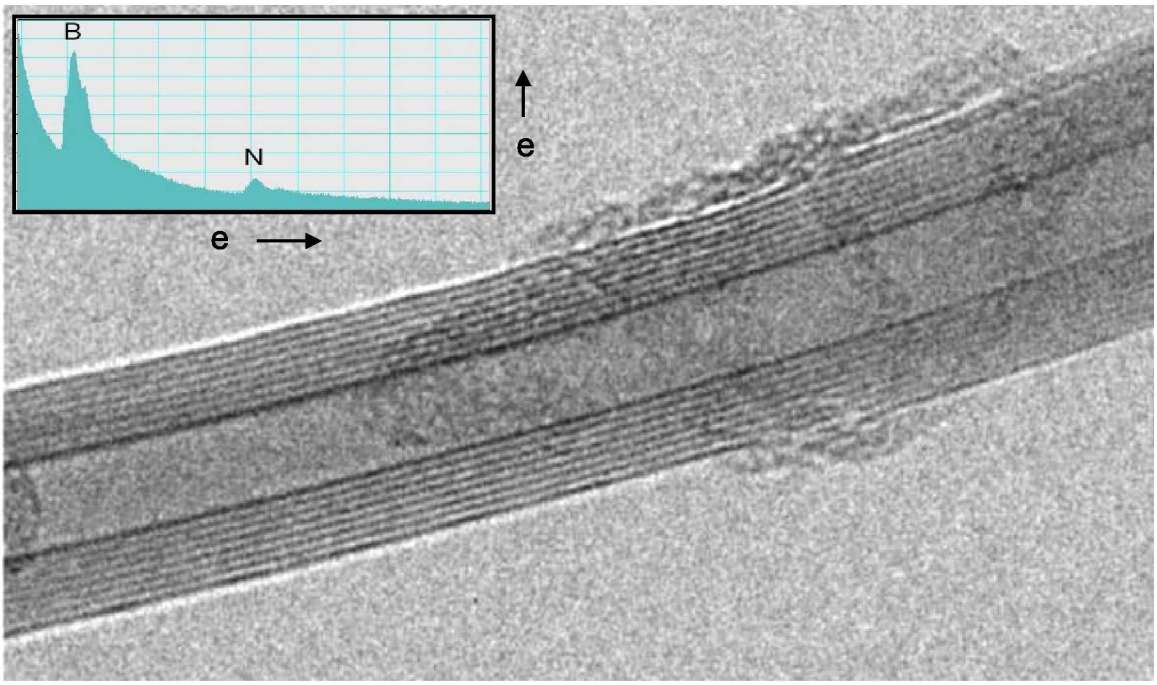

Figure 6. (A) High resolution TEM image of an 8-walled BNNT. Inset is an EELS spectrum showing 1:1 ratio of B to N.

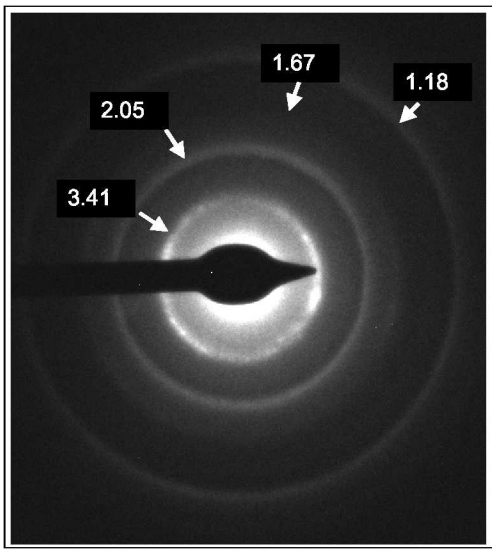

PVC--BNNTs d spacing (Å)	h-BN standard (Å)	HKL	Deviation
3.416	3.3281	{002}	2.64%
2.052	2.0619	{101}	-0.48%
1.675	1.6636	{004}	0.69%
1.183	1.1720	{112}	0.94%

Figure 7. An electron diffraction pattern for PVC-BNNTs (left side of figure), shows the major bands representing the hexagonal lattice structure. The table (right side) compares the band locations of PVC-BNNTs to those of an h-BN standard. Agreement is within 1% for all but the fundamental peak which represents the interlayer graphene spacing (~ .34 nm = 3.4 Å). This difference may be real, and due to the curvature of the h-N layers in the BNNTs relative to the planar layers in the h-BN standard.